Nonlocal theory of area-varying waves on axisymmetric vortex tubes

A. Leonard
Mail Code 301-46, Graduate Aeronautical Laboratories, California Institute of Technology, Pasadena, California 91125

(Received 20 April 1993; accepted 30 August 1993)

Area and axial flow variations on rectilinear vortex tubes are considered. The state of the flow is characterized by two dependent variables, a core area, and an azimuthal circulation per unit length, which vary in time and in distance along the length of the tube. Nonlinear integrodifferential equations of motion for these variables are derived by taking certain integrals of the vorticity transport equation. The equations are argued to be valid for moderately short waves (on the order of a few core radii) as well as for long waves. Applications to vortex breakdown and other wave phenomena are considered.

I. INTRODUCTION

In a number of applications, a three-dimensional vortical flow can be represented by a collection of vortex tubes or vortex filaments, e.g., pulsed round jets, aircraft trailing vortices, and interacting vortex rings. If the internal structure of the filament is assumed fixed, then one need only to track the space curves of the filaments in time to simulate the flow. This is done typically using Lagrangian markers and the Biot–Savart law with a suitable cutoff.[1] In this way rather complex flows can be simulated with a relatively small number of degrees of freedom.

However, the assumption of constant core structure is suspect, considering the differing stretching rates that are likely to be experienced by various Lagrangian elements of the filaments. Thus, it seems reasonable to allow for a time-dependent core diameter that varies along each filament. To be consistent one must also allow for a time- and position-dependent azimuthal vorticity component along the filaments to account for the development of helical vortex lines caused by the differential rotation rates of nominally axial vortex lines around the core center.

To account for these variations one could employ a more intensive computational approach such as using a number computational filaments per physical vortex tube[2] or a vortex particle method.[3] However, in this paper we consider a more theoretically oriented approach, that of adding two additional independent variables to account for the possibility of area variations and axial flow or azimuthal circulation variations along the vortex tube. Moore and Saffman[4] (hereinafter referred to as MS) have carried out such a development by applying conservation of momentum to a differential length of the filament and making a rather intricate determination of the forces on the filament. The result was dynamical equations for the motion of the three-dimensional space curve of the filament and for an axial flow along the tube. A similar approach was carried out by Widnall and Bliss[5] to study the evolution of general sinusoidal perturbations of a vortex filament and of a perturbed vortex pair. In both cases, the assumption was made that variations in the axial flow along the filament had length scales much larger than the core radius. In MS it was argued that any short wave variations along the filament would be smoothed out on time scales much shorter than those of interest. More recently, Lundgren and Ashurst[6] (hereinafter referred to as LA) present a derivation of vortex tube dynamics with internal structure, along the lines of MS. However, they consider applications involving short wave, short time behavior, and therefore retain a number of terms discarded by MS. In particular, they discuss the application to axisymmetric vortex breakdown in which the equations reduce to a pair of hyperbolic equations. Consequently, vortex breakdown is manifested as a "shock" or discontinuous solution. However, as LA acknowledge, the equations they use are questionable for short wave phenomena and so should be considered as model equations. They also note the close analogy with the application of the shallow water equations to hydraulic jumps.

In a related effort, Marshall[7] derives equations of motion for curved vortex filaments with variable core area and axial flow using a one-dimensional continuum model for the filament. This structure, referred to as a directed vortex filament, has its own balance laws and constitutive equations that account for part of the kinematics and dynamics of the filament. The additional information required is the external forces on the vortex that are computed *à la* MS. Some dispersive terms appear in the derivation allowing, e.g., the development of solitary waves, although the validity of the analysis is limited to long waves. Dispersive effects also arise in Leibovich's study[8] of weakly nonlinear axisymmetric waves on a vortex filament. He finds that, at the lowest order, the disturbance amplitude satisfies the Korteweg–de Vries (KdV) equation when the filament occupies the center of a cylindrical vessel. When the radius of the vessel goes to infinity a nonlocal, integral term must be added to the KdV equation.

In this paper we consider area waves on vortex tubes from the point of view of vorticity–velocity relationships. We first determine expressions for the vorticity and velocity fields in which the vorticity field is represented by a collection of space curves with area and azimuthal circulation per unit length varying along the length of each tube. We then derive equations of motion for these quantities for the case of axisymmetric flow, taking appropriate cross-sectional integrals of the vorticity transport equation. The equations include nonlocal terms, i.e., velocities that include influences at a distance through the Biot–Savart law, and are argued to be valid for moderately short waves. Relations with previous work are discussed and selected

 1070-6631/94/6(2)/765/13/$6.00

numerical computations of wave development and interaction illustrate the implications of the nonlocal terms.

II. KINEMATICS OF THREE-DIMENSIONAL VORTEX TUBES

We consider the vorticity field represented by a single vortex tube. A clear generalization is to superpose a collection of tubes or filaments. The centerline of the vortex tube lies along the space curve defined by $\mathbf{r}(\xi,t)$ where ξ is a parameter that runs along the curve. We decompose the vorticity field within the tube into two components, $\boldsymbol{\omega}_1$ and $\boldsymbol{\omega}_2$, where $\boldsymbol{\omega}_1$ is primarily axial and radial with respect to the local tangent, $\partial\mathbf{r}/\partial\xi$, and $\boldsymbol{\omega}_2$ is primarily azimuthal. In particular, $\boldsymbol{\omega}_1$ has the representation

$$\boldsymbol{\omega}_1(\mathbf{x})=\Gamma\int\frac{1}{\sigma(\xi)^3}p_1\left(\frac{|\mathbf{x}-\mathbf{r}(\xi)|}{\sigma(\xi)}\right)\left(\frac{\partial\mathbf{r}}{\partial\xi}+\frac{\mathbf{x}-\mathbf{r}(\xi)}{\sigma(\xi)}\frac{\partial\sigma}{\partial\xi}\right)d\xi, \tag{1}$$

where the function p_1 determines the distribution of the axial vorticity over the core of the tube. The variable σ plays the role of the local tube radius. For clarity, we have suppressed explicit reference to the time dependence of $\boldsymbol{\omega}_1$, σ, and $\mathbf{r}$. The term proportional to $\partial\sigma/\partial\xi$ in the integrand above yields primarily radial vorticity, and is precisely that required to satisfy $\nabla\cdot\boldsymbol{\omega}_1=0$.

We represent the azimuthal vorticity by

$$\boldsymbol{\omega}_2(\mathbf{x})=2\pi\int\frac{1}{\sigma(\xi)^3}p_2\left(\frac{|\mathbf{x}-\mathbf{r}(\xi)|}{\sigma(\xi)}\right)\times\left(\frac{\partial\mathbf{r}}{\partial\xi}\times[\mathbf{x}-\mathbf{r}(\xi)]\right)\gamma(\xi)d\xi, \tag{2}$$

where p_2 determines the distribution of azimuthal vorticity over the core. The functions p_1 and p_2 satisfy the normalization

$$4\pi\int_0^\infty p_i(r)r^2\,dr=1,\quad i=1,2. \tag{3}$$

The variable γ is also time dependent, and, as we shall see below, is approximately the circulation per unit length of azimuthal vorticity. One can verify that this component of $\boldsymbol{\omega}$ is also solenoidal, i.e., $\nabla\cdot\boldsymbol{\omega}_2=0$.

The total vorticity field is then given by

$$\boldsymbol{\omega}(\mathbf{x})=\boldsymbol{\omega}_1(\mathbf{x})+\boldsymbol{\omega}_2(\mathbf{x}). \tag{4}$$

The vector streamfunction $\boldsymbol{\psi}$ is given by the solution to

$$\nabla^2\boldsymbol{\psi}=-\boldsymbol{\omega} \tag{5}$$

or

$$\boldsymbol{\psi}(\mathbf{x})=\frac{1}{4\pi}\int\frac{\boldsymbol{\omega}(\mathbf{x}')d\mathbf{x}'}{|\mathbf{x}-\mathbf{x}'|}. \tag{6}$$

The velocity field may be determined by

$$\mathbf{u}(\mathbf{x})=\nabla\times\boldsymbol{\psi} \tag{7a}$$

or

$$\mathbf{u}(\mathbf{x})=-\frac{1}{4\pi}\int\frac{(\mathbf{x}-\mathbf{x}')\times\boldsymbol{\omega}(\mathbf{x}')d\mathbf{x}'}{|\mathbf{x}-\mathbf{x}'|^3}. \tag{7b}$$

We define components of $\boldsymbol{\psi}$ and $\mathbf{u}$, $\boldsymbol{\psi}_1$, $\boldsymbol{\psi}_2$ and $\mathbf{u}_1$, $\mathbf{u}_2$, corresponding, respectively, to $\boldsymbol{\omega}_1$, $\boldsymbol{\omega}_2$. Using (1), (2), (4), and (6), we find that

$$\boldsymbol{\psi}_1(\mathbf{x})=\frac{\Gamma}{4\pi}\int P_1\left(\frac{|\mathbf{x}-\mathbf{r}(\xi)|}{\sigma(\xi)}\right)\frac{\partial\mathbf{r}}{\partial\xi}\frac{d\xi}{\sigma}+\frac{\Gamma}{4\pi}\int Q_1\left(\frac{|\mathbf{x}-\mathbf{r}(\xi)|}{\sigma(\xi)}\right)\left(\frac{\mathbf{x}-\mathbf{r}(\xi)}{\sigma(\xi)}\right)\frac{\partial\sigma}{\partial\xi}\frac{d\xi}{\sigma} \tag{8}$$

and

$$\boldsymbol{\psi}_2(\mathbf{x})=\frac{1}{2}\int\frac{\partial\mathbf{r}}{\partial\xi}\times\left(\frac{\mathbf{x}-\mathbf{r}(\xi)}{\sigma(\xi)}\right)Q_2\left(\frac{|\mathbf{x}-\mathbf{r}(\xi)|}{\sigma(\xi)}\right)\gamma(\xi)d\xi, \tag{9}$$

where

$$P_1(y)=4\pi\left(\frac{1}{y}\int_0^y x^2p_1(x)dx+\int_y^\infty xp_1(x)dx\right), \tag{10a}$$

$$Q_i(y)=\frac{4\pi}{3}\left(\frac{1}{y^3}\int_0^y x^4p_i(x)dx+\int_y^\infty xp_i(x)dx\right),\quad i=1,2. \tag{10b}$$

The velocity components are then given by

$$\mathbf{u}_1=-\frac{\Gamma}{4\pi}\int\frac{[\mathbf{x}-\mathbf{r}(\xi)]\times(\partial\mathbf{r}/\partial\xi)f[|(\mathbf{x}-\mathbf{r}(\xi)|/\sigma(\xi)]d\xi}{|\mathbf{x}-\mathbf{r}(\xi)|^3} \tag{11}$$

and

$$\mathbf{u}_2=\int\frac{[g[|\mathbf{x}-\mathbf{r}(\xi)|/\sigma(\xi)](\partial\mathbf{r}/\partial\xi)-h[|\mathbf{x}-\mathbf{r}(\xi)|/\sigma(\xi)][\partial\mathbf{r}/\partial(\xi)]|_\perp]\sigma(\xi)^2\gamma(\xi)d\xi}{|\mathbf{x}-\mathbf{r}(\xi)|^3}, \tag{12}$$

where

$$f(y)=4\pi\int_0^y p_1(x)x^2\,dx, \tag{13a}$$

$$g(y)=y^3Q_2(y), \tag{13b}$$

$$h(y)=2\pi\int_0^y p_2(x)x^4\,dx, \tag{13c}$$

and

$$\left.\frac{\partial \mathbf{r}}{\partial \xi}\right|_{\perp}=\frac{\mathbf{x}-\mathbf{r}(\xi)}{|\mathbf{x}-\mathbf{r}(\xi)|}\times\left(\frac{\partial \mathbf{r}}{\partial \xi}\times\frac{\mathbf{x}-\mathbf{r}(\xi)}{|\mathbf{x}-\mathbf{r}(\xi)|}\right). \tag{13d}$$

For a rectilinear vortex tube, lying along the x axis, with a constant core diameter, the axial vorticity distribution is

$$\boldsymbol{\omega}_1(\mathbf{x})=\Gamma\frac{\zeta_1(r/\sigma)}{\sigma^2}\hat{e}_x, \tag{14}$$

and, with constant γ, the azimuthal vorticity field reduces to

$$\boldsymbol{\omega}_2(\mathbf{x})=\gamma\frac{2\pi r}{\sigma^2}\zeta_2\left(\frac{r}{\sigma}\right)\hat{e}_\theta, \tag{15}$$

where

$$\zeta_i(y)=\int_{-\infty}^{\infty}p_i[(x^2+y^2)^{1/2}]dx,\quad i=1,2. \tag{16}$$

Equation (16) may be inverted by taking the one-dimensional Fourier transform and then using an inverse Hankel transform, with the result

$$p_i(y)=-\frac{1}{\pi}\int_y^{\infty}\frac{d\zeta_i/dx\,dx}{\sqrt{x^2-y^2}},\quad i=1,2. \tag{17}$$

For example, the solid-body rotation core[3] and the Gaussian core give, respectively,

$$\zeta_1(y)=\begin{cases}\dfrac{1}{\pi}, & y\leqslant 1\\ 0, & y>1\end{cases}\rightarrow p_1(y)=\begin{cases}\dfrac{1}{\pi^2\sqrt{1-y^2}}, & y<1,\\ 0, & y>1,\end{cases} \tag{18a}$$

and

$$\zeta_1(y)=\frac{\exp(-y^2)}{\pi}\rightarrow p_1(y)=\frac{\exp(-y^2)}{\pi^{3/2}}. \tag{18b}$$

Because of the normalization condition on p_i (3), ζ_i satisfies $\int_0^{\infty}2\pi\zeta_i(x)x\,dx=1$, so that for a rectilinear vortex with constant σ, γ,

$$\int_0^{\infty}\boldsymbol{\omega}_1(\mathbf{x})2\pi r\,dr=\Gamma\hat{e}_x, \tag{19}$$

as required, and

$$\int_0^{\infty}\boldsymbol{\omega}_2(\mathbf{x})dr=\gamma\hat{e}_\theta. \tag{20}$$

Hence, γ is the circulation/length of azimuthal vorticity and

$$\mathbf{u}_2(\mathbf{x})=\gamma\left(1-\int_0^{r/\sigma}2\pi x\zeta_2(x)dx\right)\hat{e}_x. \tag{21}$$

In addition, we have that

$$\mathbf{u}_1(\mathbf{x})=\frac{\Gamma}{r}\left(\int_0^{r/\sigma}x\zeta_1(x)dx\right)\hat{e}_\theta. \tag{22}$$

III. DYNAMICAL EQUATIONS FOR AXISYMMETRIC FLOWS

We now consider the case of a rectilinear vortex tube, but with variable cross section and variable axial flow. Thus, we need to derive equations of motion for σ and γ. Our starting point is the vorticity transport equation for axisymmetric flow,

$$\frac{\partial\omega_\theta}{\partial t}+\frac{\partial}{\partial x}(u_x\omega_\theta)+\frac{\partial}{\partial r}(u_r\omega_\theta)=-\frac{2\omega_r u_\theta}{r}, \tag{23}$$

$$\frac{\partial\omega_x}{\partial t}+\frac{1}{r}\frac{\partial}{\partial r}[r(u_r\omega_x-u_x\omega_r)]=0. \tag{24}$$

The component ω_r may be computed from ω_x using $\nabla\cdot\boldsymbol{\omega}=0$. Our strategy is to derive suitable expressions for the velocity and vorticity components, using (1), (2), (11), and (12), and substitute them into (23) and (24) above. Taking certain moments in r of the equations will lead to the desired equations for σ and γ. This is equivalent to a low-order weighted residual method to treat the r dependence in the governing equations, but perhaps it is better to think of the procedure as an integral method. In addition, we will see that a particular choice of the distribution function for the azimuthal vorticity, p_2, given the distribution p_1, appears to minimize the error.

Assuming that $p_1(y)$ and $p_2(y)$ decay rapidly for $y>1$, as in (18a) and (18b), and that variations in σ and γ do not have length scales on the order of σ, we can use "local" approximations for the vorticity components as follows:

$$\omega_x\approx\frac{\Gamma\zeta_1[r/\sigma(x)]}{\sigma^2(x)}, \tag{25}$$

$$\omega_r\approx\frac{\Gamma r}{\sigma}\frac{\partial\sigma}{\partial x}\frac{\zeta_1[r/\sigma(x)]}{\sigma^2(x)}, \tag{26}$$

$$\omega_\theta\approx\frac{2\pi r}{\sigma^2(x)}\zeta_2\left(\frac{r}{\sigma(x)}\right)\gamma(x). \tag{27}$$

In addition, for axisymmetric flow, u_θ is simply related to ω_x. The approximation (25) therefore gives the "local" approximation for u_θ,

$$u_\theta\approx\frac{\Gamma}{r}\left(\int_0^{r/\sigma(x)}y\zeta_1(y)dy\right). \tag{28}$$

On the other hand, u_x and u_r are "nonlocal" variables, in that the contribution at x to u_x and u_r of $\gamma(x')dx'$ do not decay rapidly. In particular, these contributions, du_x and du_r, for $|x-x'|\gg\sigma(x')$, are given by (12) as

$$d\mathbf{u}_2=\frac{8\pi}{3}\left(\int_0^{\infty}y^4p_2(y)dy\right)\sigma^2(x')\gamma(x')dx'\times\left[\left(\frac{1}{[(x-x')^2+r^2]^{3/2}}-\frac{3r^21}{2[(x-x')^2+r^2]^{5/2}}\hat{e}_x\right)+\frac{3r(x-x')\hat{e}_r}{2[(x-x')^2+r^2]^{5/2}}\right]. \tag{29}$$

The above expression is equivalent to the far field of a vortex ring at x' of circulation $d\Gamma$ and ring radius R with

$$R^2=\frac{16\pi}{3}\left(\int_0^{\infty}y^4p_2(y)dy\right)\sigma^2(x')$$

and

$$d\Gamma=\gamma(x')dx'.$$

In general, for axisymmetric flow, (9) reduces to

$$\psi_2=\psi_\theta\hat{e}_\theta, \tag{30a}$$

where

$$\psi_\theta(x,r)=\frac{r}{2}\int_{-\infty}^{\infty}Q_2\left(\frac{[(x-x')^2+r^2]^{1/2}}{\sigma(x')}\right)\frac{\gamma(x')dx'}{\sigma(x')}, \tag{30b}$$

and u_x and u_r are given by

$$u_x=\frac{1}{r}\frac{\partial}{\partial r}(r\psi_\theta), \tag{31a}$$

$$u_r=-\frac{\partial}{\partial x}\psi_\theta. \tag{31b}$$

Note that the source term for azimuthal vorticity, given by the RHS of (23), is

$$\frac{-2\omega_x u_\theta}{r}=-\frac{\Gamma^2}{\pi\sigma^4}\frac{\partial\sigma}{\partial x}\left(\frac{\zeta_1(z)2\pi\int_0^z y\zeta_1(y)dy}{z}\right)_{z=r/\sigma(x)}, \tag{32}$$

using (26) and (28), while the first term on the LHS of (23) is given by

$$\frac{\partial\omega_\theta}{\partial t}=\frac{2\pi}{\sigma(x)}\frac{\partial\gamma}{\partial t}[z\zeta_2(z)]_{z=r/\sigma}+[\cdots]\frac{\partial\sigma}{\partial t}. \tag{33}$$

Thus, we can match the r dependence of the $\partial\gamma/\partial t$ term and the source term by choosing

$$\zeta_2(z)=\frac{C\zeta_1(z)2\pi\int_0^z y\zeta_1(y)dy}{z^2}, \tag{34}$$

where C is the constant required to satisfy the normalization condition on p_2, or, equivalently, on ζ_2. For solid-body rotation and therefore ζ_1 given by (18a), we find $\zeta_2=\zeta_1$ and $C=1$. For the Gaussian core,

$$\zeta_2(z)=\frac{1}{\pi\log(2)z^2}[\exp(-z^2)-\exp(-2z^2)] \tag{35a}$$

and

$$C=\frac{1}{\log(2)}. \tag{35b}$$

An evolution equation for γ follows from (23) by substituting the expressions for the velocity and vorticity components (25)–(28) into (23) and integrating over the r coordinate, $\int_0^\infty$[Eq. (23)]$dr=0$. This gives the result

$$\frac{\partial\gamma}{\partial t}+\frac{\partial}{\partial x}(q\gamma)=-\frac{\Gamma^2}{2\pi^2C\sigma^3}\frac{\partial\sigma}{\partial x}, \tag{36}$$

where $q(x)$ is the following average of $u_x(r,x)$:

$$q=\int_0^\infty\frac{2\pi r}{\sigma(x)^2}\zeta_2\left(\frac{r}{\sigma(x)}\right)u_x(r,x)dr, \tag{37}$$

i.e., u_x weighted by ω_θ over r. Using (30b), (31a), and (37) gives the required relation between q and the distribution of circulation γ as follows:

$$q=\int_{-\infty}^{\infty}K\left(\frac{|x-x'|}{\sigma(x')},\frac{\sigma(x)}{\sigma(x')}\right)\frac{\gamma(x')dx'}{\sigma(x')}, \tag{38}$$

where

$$K(x,y)=-\pi\int_0^\infty z^2\frac{d\zeta_2(z)}{dz}Q_2[(x^2+z^2y^2)^{1/2}]dz. \tag{39}$$

For the constant-vorticity core,

$$K\left(\frac{|x-x'|}{\sigma(x')},\frac{\sigma(x)}{\sigma(x')}\right)=Q_2\left[\left(\frac{(x-x')^2+\sigma(x)^2}{\sigma(x')^2}\right)^{1/2}\right]. \tag{40}$$

Taking the zeroth r moment of Eq. (23), as we have done, yields a relatively simple evolution equation for γ and corresponds to imposing conservation of azimuthal circulation. Taking the second moment, $\int_0^\infty$[Eq. (23)]$r^2\,dr=0$, is closely related to imposing the conservation of x momentum, but leads to a more complicated dynamical equation.

To obtain a dynamical equation for σ^2, we consider the transport equation for ω_x. The first moment, $\int_0^\infty$[Eq. (24)]$r\,dr=0$, simply leads to $d\Gamma/dt=0$. However, the third moment, $\int_0^\infty$[Eq. (24)]$r^3\,dr=0$, expressing conservation of angular momentum, yields

$$\frac{\partial\sigma^2}{\partial t}+\frac{\partial}{\partial x}(\tilde{q}\sigma^2)=0, \tag{41}$$

where $\tilde{q}$ is the planar-averaged $u_x(r,x)$ weighted by the "excess" angular momentum, $ru_\theta-\Gamma/2\pi$,

$$\tilde{q}(x)=\frac{\int_0^\infty(ru_\theta-\Gamma/2\pi)u_x2\pi r\,dr}{\int_0^\infty(ru_\theta-\Gamma/2\pi)2\pi r\,dr}. \tag{42}$$

In terms of σ and γ, $\tilde{q}$ is given by

$$\tilde{q}=\int_{-\infty}^{\infty}\tilde{K}\left(\frac{|x-x'|}{\sigma(x')},\frac{\sigma(x)}{\sigma(x')}\right)\frac{\gamma(x')dx'}{\sigma(x')}, \tag{43}$$

where

$$\tilde{K}(x,y)=\frac{\int_0^\infty z^3\zeta_1(z)Q_2[(x^2+z^2y^2)^{1/2}]dz}{\int_0^\infty z^3\zeta_1(z)dz}. \tag{44}$$

The kernel $\tilde{K}$ for a constant-vorticity core is given in the Appendix. Here K and $\tilde{K}$ have the expected behavior,

$$K,\tilde{K}\to O\left(\frac{1}{|x-x'|^3}\right),\quad\text{if } |x-x'|\gg\sigma(x').$$

If γ and σ are slowly varying in x, i.e., variations consist of length scales λ such that $\lambda\gg\sigma$, then we can make the zeroth-order approximation

$$\gamma(x')\approx\gamma(x), \tag{45a}$$

$$\sigma(x')\approx\sigma(x), \tag{45b}$$

in (38) and (43), and obtain, for the constant vorticity core,

$$q(x)\approx\tfrac{1}{2}\gamma(x), \tag{46a}$$

$$\tilde{q}(x)\approx\tfrac{2}{3}\gamma(x). \tag{46b}$$

This approximation yields hyperbolic equations for γ and σ,

$$\frac{\partial\gamma}{\partial t}+\frac{1}{2}\frac{\partial\gamma^2}{\partial x}=-\frac{\Gamma^2}{2\pi^2\sigma^3}\frac{\partial\sigma}{\partial x}, \tag{47a}$$

$$\frac{\partial\sigma^2}{\partial t}+\frac{2}{3}\frac{\partial}{\partial x}(\gamma\sigma^2)=0. \tag{47b}$$

Except for multiplicative constants, the above equations are identical to those derived by LA when their equations are reduced for the case of one-dimensional flow (Sec. IV). In their case, γ is the local axial velocity assuming slug flow. The constants differ because of the differences in assumed velocity profiles. In their derivation, as in the derivation of MS, it is assumed that the pressure is the solution to the approximate radial momentum equation, neglecting radial acceleration,

$$\frac{\partial p}{\partial r}=\frac{\rho u_\theta^2}{r},$$

with the result that the pressure is determined locally because u_θ is a local variable. Thus, in LA, Eq. (47a) is arrived at via the axial momentum equation, with the RHS the pressure derivative term. They suggest that an improvement could be obtained by including an approximation for the radial acceleration in the radial momentum equation. In a sense this improvement is accomplished in the present analysis, but through vorticity–velocity kinematics rather than pressure–velocity relationships.

IV. LINEAR AND NONLINEAR WAVES

We return to the original equations, (36), (38), (41), and (43), presumably valid for moderately short ($\lambda\gtrsim\sigma$) as well as long waves, and derive the dispersion relation for linear, sinusoidal perturbations on a filament with constant radius and constant axial flow. We therefore assume

$$\sigma^2(x,t)=\sigma_0^2+\sigma^{2\prime}\exp[i(kx-\omega t)], \tag{48a}$$

$$\gamma(x,t)=\gamma_0+\gamma'\exp[i(kx-\omega t)], \tag{48b}$$

with

$$\sigma^{2\prime}\ll\sigma_0^2$$

$$|\gamma'|\ll\max\left(|\gamma_0|,\frac{\Gamma}{2\pi\sigma_0}\right).$$

We also assume that the unperturbed filament has a constant vorticity core. Substituting (48) into (36) and (38) and linearizing gives

$$\left(-c+\frac{\gamma_0}{2}[1+F(k\sigma_0)]\right)\gamma'+\left(\frac{\gamma_0^2}{2}[F(k\sigma_0)-1]+\frac{\Gamma^2}{4\pi^2\sigma_0^2}\right)\frac{\sigma^{2\prime}}{\sigma_0^2}=0, \tag{49a}$$

and, similarly, (41) and (43) lead to

$$\left(\frac{2}{3}G_1(k\sigma_0)\right)\gamma'+\left(-c+\frac{\gamma_0}{3}[1-G_1(k\sigma_0)]+\frac{2\gamma_0}{3}G_2(k\sigma_0)\right)\times\frac{\sigma^{2\prime}}{\sigma_0^2}=0, \tag{49b}$$

where

$$c=\omega/k, \tag{50a}$$

$$F(z)=zK_1(z), \tag{50b}$$

$$G_1(z)=6\int_0^1 y^3\,dy\int_{-\infty}^{\infty}Q_2[(x^2+y^2)^{1/2}]e^{izx}\,dx, \tag{50c}$$

$$G_2(z)=-3\int_0^1 y^3\,dy\int_{-\infty}^{\infty}Q_2'[(x^2+y^2)^{1/2}]\times(x^2+y^2)^{1/2}e^{izx}\,dx, \tag{50d}$$

and K_1 is the modified Bessel function. For a nontrivial solution to (49) and for a given σ_0^2, γ_0, and k, the wave speed c must satisfy

$$c=\gamma_0\left[\tfrac{7}{12}+F(k\sigma_0)/4+\tfrac{1}{6}[2G_2(k\sigma_0)-G_1(k\sigma_0)-1)]\right.$$
$$\left.\pm\sqrt{\frac{\gamma_0^2}{4}\left(\frac{F(k\sigma_0)}{2}-\frac{1}{6}-\frac{1}{3}[2G_2(k\sigma_0)-G_1(k\sigma_0)-1]\right)^2+\frac{\gamma_0^2}{3}G_1(k\sigma_0)(F(k\sigma_0)-1)+\frac{\Gamma^2G_1(k\sigma_0)}{6\pi^2\sigma_0^2}}\right. \tag{51}$$

The functions F, G_1, G_2 all satisfy $F(0)=G_1(0)=G_2(0)=1$, so that in the limit of zero wave number,

$$c|_{k=0}=\frac{5}{6}\gamma_0\pm\sqrt{\frac{\gamma_0^2}{36}+\frac{\Gamma^2}{6\pi^2\sigma_0^2}}. \tag{52}$$

For the constant vorticity core, $Q_2(z)=1/(4z^3)$ if $z>1$. This gives the result

$$G_1(z)=1+\tfrac{3}{8}z^2\ln(z/2)+O(z^2), \tag{53}$$

so that, if $\gamma_0=0$, we find for the long wave limit,

$$c=\pm\frac{\Gamma\sqrt{G_1(k\sigma_0)}}{\sqrt{6}\pi\sigma_0},$$

$$=\pm\frac{\Gamma}{\sqrt{6}\pi\sigma_0}\left(1+\frac{3}{16}(k\sigma_0)^2\ln\frac{(k\sigma_0)}{2}+O(k^2\sigma_0^2)\right) \tag{54a}$$

$$=\pm\frac{\Gamma}{2.449,\cdots\pi\sigma_0}\left[1+0.1875(k\sigma_0)^2\ln\left(\frac{k\sigma_0}{2}\right)+O(k^2\sigma_0^2)\right]. \tag{54b}$$

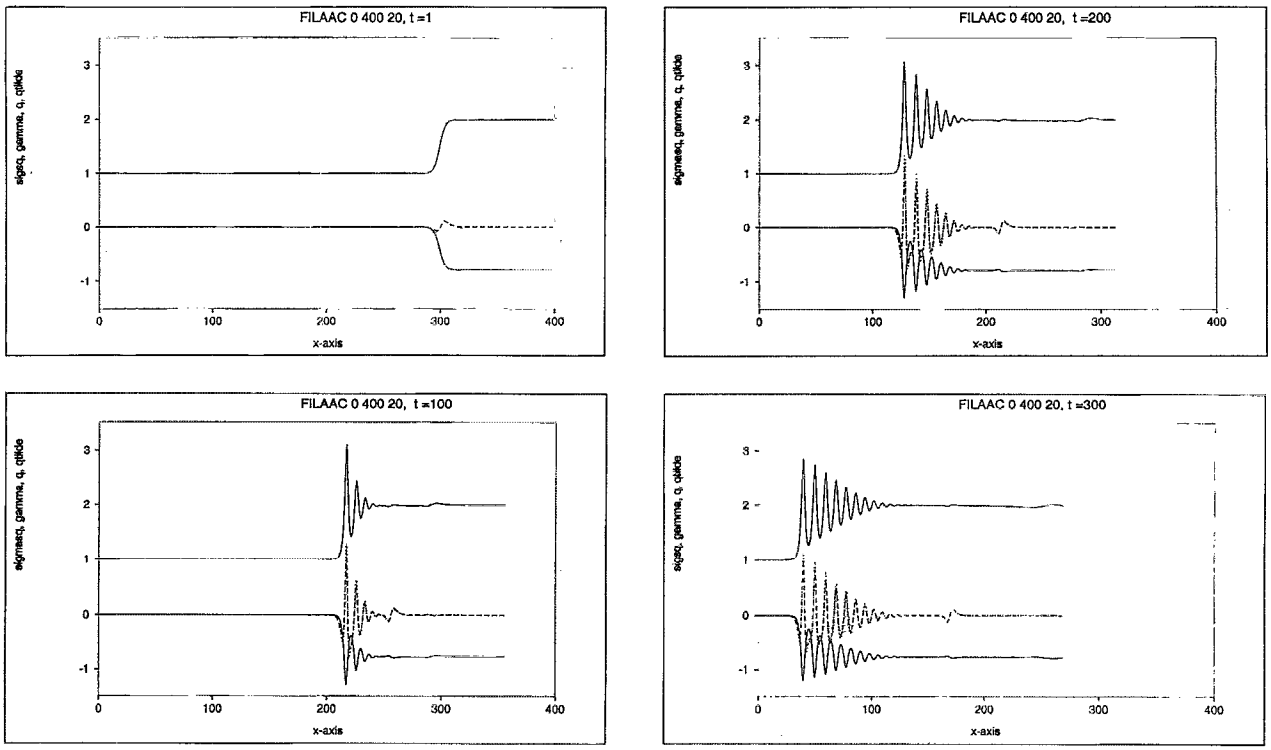

FIG. 1. Evolution of two adjacent, initially constant states. Here $\sigma_1^2=1$, $\gamma_1=0$, $\sigma_2^2=2$, and $\gamma^2=\gamma_{2\_}$ computed from (59b). We see $\sigma^2(x,t)$ —— (upper); $\gamma(x,t)$ — (lower); $10[q(x,t)-\frac{1}{2}\gamma(x,t)]$, ---; $10[\tilde{q}(x,t)-\frac{2}{3}\gamma(x,t)]$, $\cdots$.

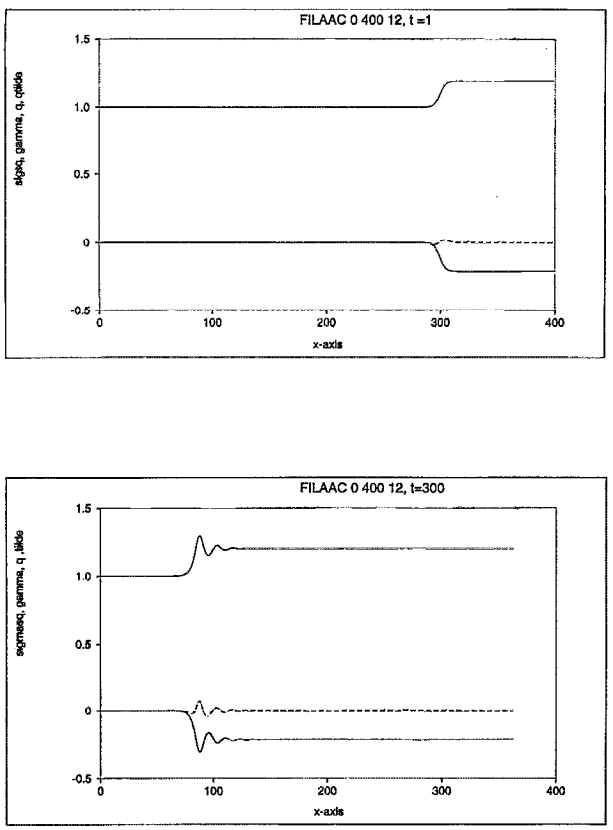

FIG. 2. Evolution of two adjacent, initially constant states. Here $\sigma_1^2=1$, $\gamma_1=0$, $\sigma_2^2=1.2$, and $\gamma_2=\gamma_{2\_}$ computed from (59b). The legend is the same as in Fig. 1.

The exact dispersion equation for this case ($\gamma_0=0$, constant-vorticity core) was determined by Kelvin[9] to be

$$\frac{1}{\beta\sigma_0}\frac{J_0'(\beta\sigma_0)}{J_0(\beta\sigma_0)}=-\frac{1}{k\sigma_0}\frac{K_0'(k\sigma_0)}{K_0(k\sigma_0)}, \tag{55}$$

where

$$\beta^2=\frac{k^2[(\Gamma^2/\pi^2\sigma_0^4)-\omega^2]}{\omega^2},$$

and J_0 and K_0 are Bessel functions.

In the long-wave limit, (55) gives

$$c=\pm\frac{\Gamma}{j_{0,1}\pi\sigma_0}\left(1+\frac{1}{j_{0,1}^2}(k\sigma_0)^2\ln\left(\frac{k\sigma_0}{2}\right)+O(k^2\sigma_0^2)\right)$$

$$=\pm\frac{\Gamma}{2.4048\ldots\pi\sigma_0}\left(1+0.1729\ldots(k\sigma_0)^2\ln\frac{(k\sigma_0)}{2}\right.$$

$$\left.+O(k^2\sigma_0^2)\right), \tag{56}$$

where $j_{0,1}$ is the first zero of J_0. Equation (56) is in reasonably good agreement with result (54) from our integral method. The appearance of the term $(k\sigma_0)^2\ln(k\sigma_0)$ in (54) is a direct consequence of the far-field behavior K and $\bar{K}$ discussed above [see after Eq. (44)].

Krishnamoorthy[10] has extended Kelvin's result for a constant-vorticity vortex tube with axial flow but for uniform (slug) flow, and not the parabolic profile we assume as a good choice to match the r dependences of the source term and the time derivative term in the ω_θ equation.

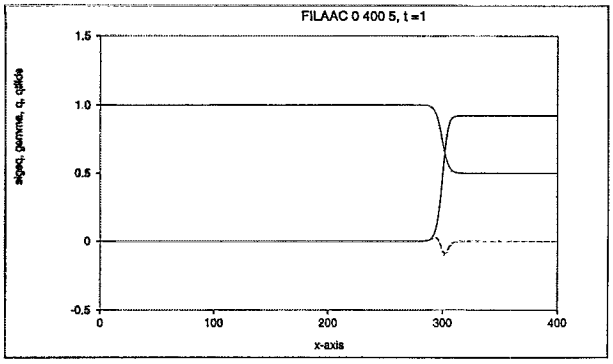

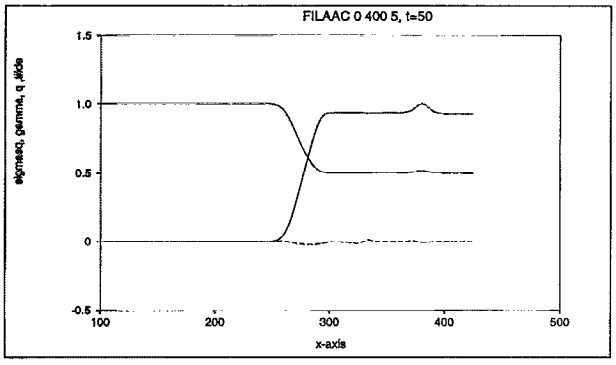

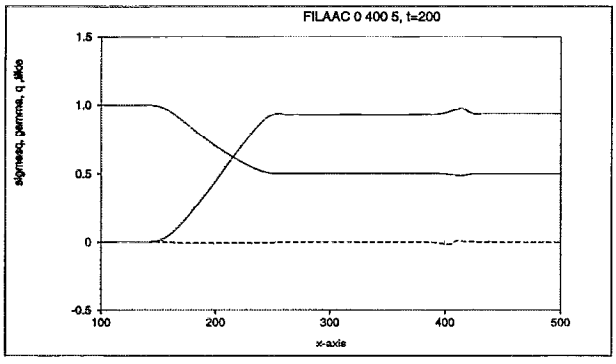

FIG. 3. Evolution of two adjacent, initially constant states. Here $\sigma_1^2=1$, $\gamma_1=0$, $\sigma_2^2=0.5$, and $\gamma_2=\gamma_{2\_}$ computed from (59b). The legend is the same as in Fig. 1.

We now consider nonlinear waves and look for traveling wave solutions of the form

$$\gamma=\gamma(x-ct),$$

$$\sigma^2=\sigma^2(x-ct).$$

In this case (36) and (41) may be integrated to obtain $\gamma(\eta)$, $\sigma^2(\eta)$, $\eta=x-ct$, as follows:

$$[-c+q(\eta)]\gamma-\frac{\Gamma^2}{4\pi^2\sigma^2}=\left(-c+\frac{1}{2}\gamma_1\right)\gamma_1-\frac{\Gamma}{4\pi^2\sigma_1^2}, \tag{57a}$$

$$[-c+\tilde{q}(\eta)]\sigma^2=(-c+\tfrac{2}{3}\gamma_1)\sigma_1^2, \tag{57b}$$

where q and $\tilde{q}$ are given by (38) and (43), respectively, with η, η' replacing x,x'. The right-hand sides above are the constants of integration evaluated at an assumed constant asymptotic state 1.

If we assume that adjacent asymptotic constant states are possible (state 1 and state 2), then from (57) we find that

$$\left(-c+\frac{1}{2}\gamma_1\right)\gamma_1-\frac{\Gamma^2}{4\pi^2\sigma_1^2}=\left(-c+\frac{1}{2}\gamma_2\right)\gamma_2-\frac{\Gamma^2}{4\pi^2\sigma_2^2}, \tag{58a}$$

$$(-c+\tfrac{2}{3}\gamma_1)\sigma_1^2=(-c+\tfrac{2}{3}\gamma_2)\sigma_2^2. \tag{58b}$$

Thus, for example, given the circulation γ_1, and area ratio, σ_1^2/σ_2^2, the wave speeds are

$$c=c_\pm=\frac{2}{3}\gamma_1+\frac{1}{f}\left(\frac{\gamma_1}{6}\pm\sqrt{\frac{\gamma_1^2}{36}+\frac{\Gamma^2 f}{6\pi^2\sigma_1^2}}\right), \tag{59a}$$

and the corresponding circulations γ_2 are

$$\gamma_2=\gamma_{2\pm}=\left(\frac{2}{3}+\frac{1}{3f}\right)\gamma_1\pm\left(\frac{2}{f}-2\right)\sqrt{\frac{\gamma_1^2}{36}+\frac{\Gamma^2 f}{6\pi^2\sigma_1^2}}, \tag{59b}$$

where

$$f=\frac{3}{4}\frac{\sigma_1^2}{\sigma_2^2}+\frac{1}{4}.$$

However, we strongly suspect that only one of the the two ($\pm$) solutions for c and γ_2 given in Eq. (59) will yield a valid transition from state 1 to state 2. If we consider the hyperbolic equation (47) corresponding to the long-wavelength approximation, then (58) gives the jump conditions for a discontinuous (shock) transition from state 1 to state 2. However, such a transition must satisfy a breaking[11] or entropy condition,[12] in that two characteristics must intersect the shock from one side and one must intersect from the other. The characteristic speeds are given by

$$\lambda_\pm=\frac{5}{6}\gamma\pm\sqrt{\frac{\gamma^2}{36}+\frac{\Gamma^2}{6\pi^2\sigma^2}}, \tag{60}$$

i.e., the same as the zero-wave number wave speeds for the linearized equations. [see (52)]. Assuming state 1 is on the left and state 2 is on the right, we find that the entropy condition is satisfied for

$$c=c_+, \quad \text{if } \sigma_1^2>\sigma_2^2,$$

and for

$$c=c_-, \quad \text{if } \sigma_1^2<\sigma_2^2,$$

where the $c_\pm$ are given by (59a), and γ_2 must be chosen correspondingly from (59b). Similar conditions were argued to be necessary by LA for their system of hyperbolic equations using the clear analogy with 1-D gas-dynamics for their equations. In either case above the side with the smaller area is the supercritical side (both characteristics intersect the shock), while the other is subcritical. We assume that these conditions remain valid for the full equa-

tions, but we expect some structure in the transition between states. In fact, we will see that the subcritical side will not consist of only an asymptotically constant state, but will have an additional wave-train component.

We note in passing that (57a) allows us to formulate a necessary condition for vortex breakdowns that have axial flow reversal on the axis, as described by the present theory in the case of steady flow. Let $c=-U_\infty$ to obtain a stationary wave, where $U_\infty(>0)$ is a constant free-stream axial velocity. Also, let $\gamma_1>0$. Then as σ_2^2 becomes large with respect to σ_1^2, the only possibility for $\gamma(\eta)$ to become negative (a necessary condition for flow reversal on the axis) is for the RHS of (57a) to be negative, i.e.,

$$\frac{\Gamma^2}{4\pi^2\sigma_1^2}>\left(U_\infty+\frac{1}{2}\gamma_1\right)\gamma_1. \tag{61a}$$

This condition appears to be analogous to the rigorous necessary condition found by Brown and Lopez,[13] based on the full Euler equations for steady axisymmetric flow. Their condition is that at constant upstream conditions the helix angle for the velocity must be greater than that of the vorticity for some stream surface. For our assumed velocity and profiles, the Brown and Lopez condition is thus given by

$$\frac{\Gamma^2}{4\pi^2\sigma_1^2}>\left[U_\infty+\left(1-\frac{r^2}{\sigma_1^2}\right)\gamma_1\right]\gamma_1, \tag{61b}$$

for some r such that $0<r<\sigma_1$. Note that (61a) is a more stringent condition.

V. NUMERICAL EXPERIMENTS

We consider the case of a constant vorticity core and choose approximations to K and $\tilde{K}$, satisfying the correct asymptotic behavior

$$K,\tilde{K}\to\frac{1}{4}\frac{\sigma^3(x')}{|x-x'|^3},\quad \text{as } |x-x'|\to\infty,$$

and the correct result if constant σ and γ were used in (38) and (43). In addition, to allow for the unusual but possible situation, $\sigma^2(x')\gg\sigma^2(x)+(x-x')^2$, we require that K, $\tilde{K}\to$const in this case. The above considerations lead to the approximate expressions for q and $\tilde{q}$:

$$q=\frac{1}{4}\int_{-\infty}^{\infty}\frac{\sigma^2(x')\gamma(x')dx'}{[(x-x')^2+\frac{1}{2}\sigma^2(x)+\frac{1}{2}\sigma^2(x')]^{3/2}}, \tag{62}$$

$$\tilde{q}=\frac{1}{4}\int_{-\infty}^{\infty}\frac{\sigma^2(x')\gamma(x')dx'}{[(x-x')^2+\frac{3}{8}\sigma^2(x)+\frac{3}{8}\sigma^2(x')]^{3/2}}. \tag{63}$$

The above expressions also preserve the long-wave expansion of the dispersion relation (54b). Then we solve numerically (36) with $C=1$ and (41) using (62) and (63). Equation (41) is solved conveniently using Lagrangian particles traveling with speed $\tilde{q}$. The quantity $\sigma^2\,\delta l$ is then conserved, where δl is the distance between particles. The azimuthal circulations of the Lagrangian particles, however, vary according to Eq. (36). This equation may be rewritten as

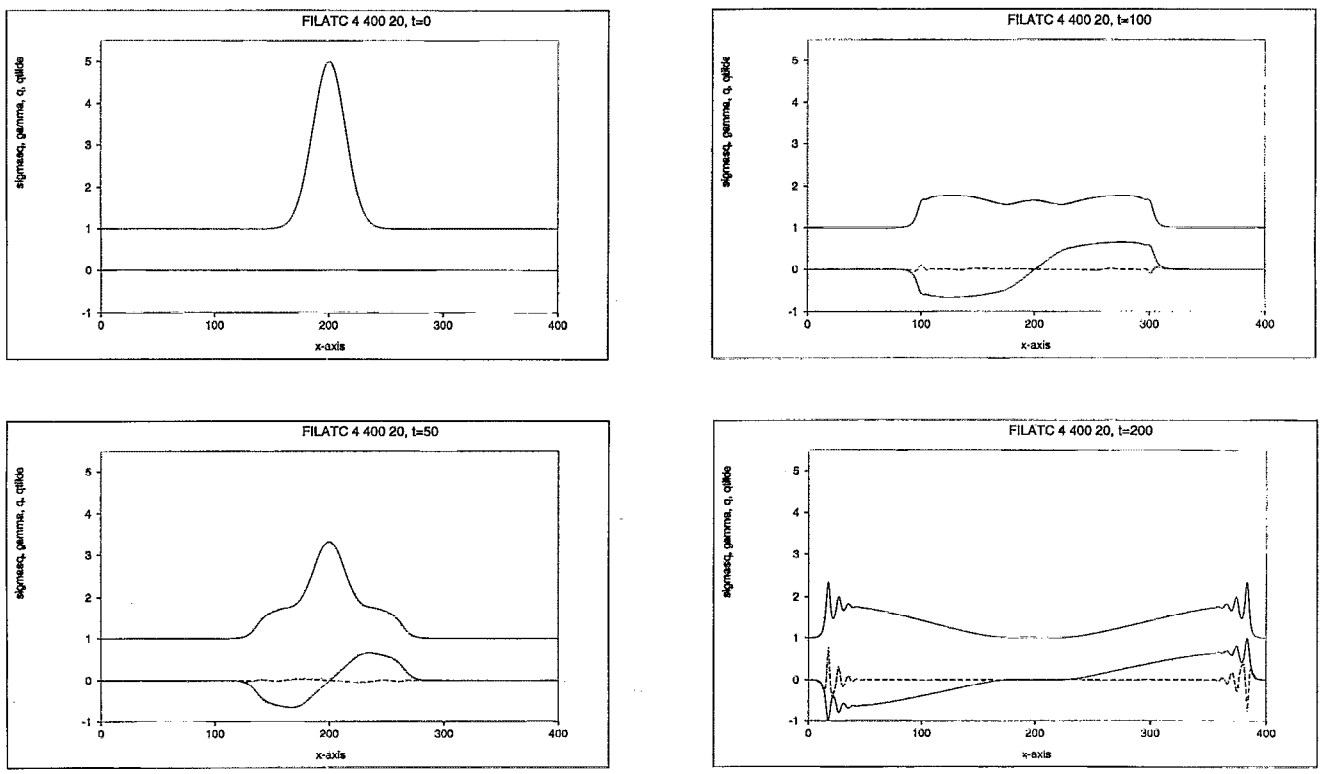

FIG. 4. Evolution of an initial area bulge. Here $\sigma^2(x,0)=1+4\exp[-(x-200)^2/400]$, $\gamma(x,0)=0$. The legend is the same as in Fig. 1.

$$\frac{\partial \gamma}{\partial t}+\frac{\partial}{\partial x}(\tilde{q}\gamma)=\frac{\partial}{\partial x}\left(\frac{\Gamma^2}{4\pi^2\sigma^2}+(\tilde{q}-q)\gamma\right). \tag{64}$$

The RHS of (64) is therefore a source of circulation for the quantity, $\gamma\,\delta l$, the circulation between adjacent Lagrangian markers.

In all cases below, $\Gamma=2\pi$ and the minimum initial $\sigma^2=1$. Time integration is by third-order Runge–Kutta, with $\Delta t=1$, and the RHS of (64) is computed by second-order central differences, with the initial spacing between Lagrangian particles=1 (except for the case shown in Fig. 9, where $\Delta t=0.5$ and the initial spacing=0.5).

No explicit artificial damping is used, even for the hyperbolic cases. Conservation of $\sigma^2\,\delta l$ gives the average σ^2 between two adjacent particles. Whenever σ^2 is required at a particle location, the average of the two σ^2's on either side is used. The integrals in (62) and (63) are computed at the particle locations by changing to Lagrangrian variables and using a midpoint-rule quadrature. However, to increase the accuracy, q and $\tilde{q}$ are not computed directly from (62) and (63). Instead, we compute $q-\frac{1}{2}\gamma$ and $\tilde{q}-\frac{2}{3}\gamma$ by subtracting

$$\frac{\sigma^2(x)\gamma(x)}{4[(x-x')^2+\sigma^2(x)]^{3/2}}$$

and

$$\frac{\sigma^2(x)\gamma(x)}{4[(x-x')^2+\frac{3}{4}\sigma^2(x)]^{3/2}},$$

from the integrands in (62) and (63), respectively.

Figure 1 shows the structure that evolves for the transition from one asymptotic constant state to another, assumed to be constant. Here the area on the right is larger, i.e., $\sigma_2^2=2\sigma_1^2$, so that the assumed constant γ_2 is equal to $\gamma_{2\_}$ given by (59b). Notice the ever increasing domain of oscillatory behavior on the subcritical side of the transition. The semi-infinite wave train that results as $t\to\infty$ corresponds directly with the wave train component on the subcritical side in Benjamin's theory of vortex breakdown based on the Bragg–Hawthorne equation.[14,15] This feature appears to be generic and analogous to the undulating motion on the subcritical side of a weak hydraulic jump. In the case of hydraulic jumps such behavior is not accessible via the shallow water equations, which are purely hyperbolic, but is found by corrections to the shallow water equations, which include dispersive effects, e.g., the KdV equation[16] or cnoidal-wave theory.[17] The triangular-shaped envelope of the oscillations, which is seen in Fig. 1 to be steadily increasing in length, is also observed in the computed solution to the KdV equation with an initial negative step.[16] However, we suspect that there exists no steady-state traveling wave of this type as $t\to\infty$, as is true in the case of the KdV equation. Benjamin's analysis leads to such a steady-state wave, but only after imposing an external "flow force" to effect the transition between states.

In Fig. 2 we show the result of a milder transition, $\sigma_2^2=1.2\sigma_1^2$, than that shown in Fig. 1. The amplitude of the wave train is, of course, smaller, but the wavelength is

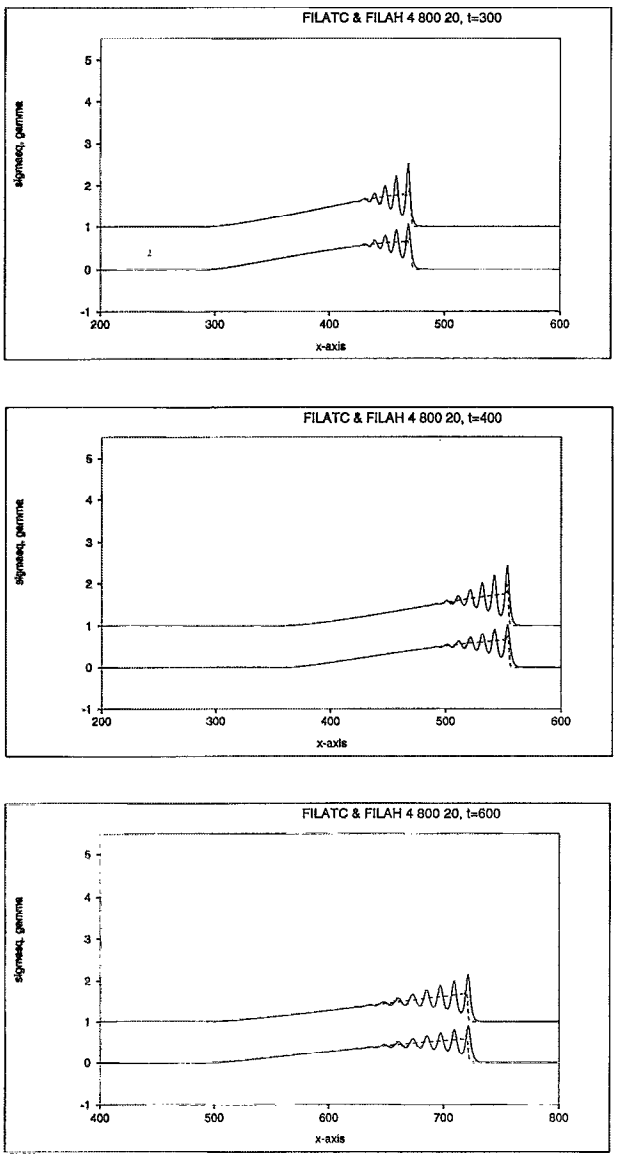

FIG. 5. Continuation of the case shown in Fig. 4, with a right traveling wave only. Solid lines, full nonlocal equations, as in Fig. 4. Dashed lines, solution to hyperbolic equations (47). Here $\sigma^2(x,t)$, upper curves; $\gamma(x,t)$, lower curves.

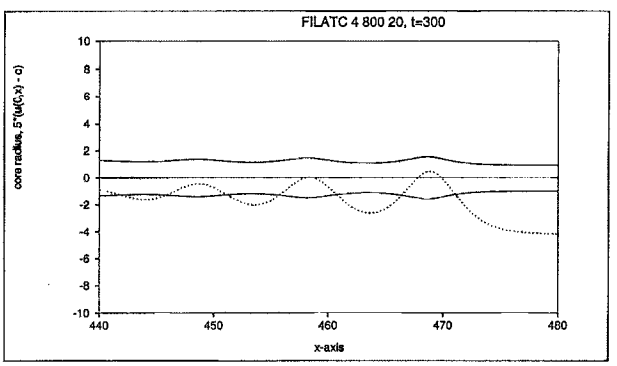

FIG. 6. The case of Fig. 4, part of the right traveling wave. Solid curves, core boundaries, and centerline. Dotted curve, $5[u(0,x)-c]$, where c=wave speed=0.84.

longer. This wavelength can be determined approximately by a perturbation calculation for $\sigma_2^2 \approx \sigma_1^2$ using (59) to find, for the case $\gamma_1 = 0$,

$$c_- \approx -\frac{\Gamma}{\sqrt{6\pi}\sigma_1}\left(1+\frac{3}{8}\epsilon\right), \tag{65a}$$

$$\gamma_{2-} \approx -\frac{\Gamma}{\sqrt{6\pi}\sigma_1}\left(\frac{3}{2}\epsilon\right), \tag{65b}$$

for

$$\sigma_2^2 = \sigma_1^2(1+\epsilon).$$

We equate the RHS of (65a) to the RHS of (51) to find the wave number k of the disturbance excited by a perturbation traveling with speed c_-. The result is

$$\epsilon \approx -\frac{1}{2}(k\sigma_1)^2 \ln\left(\frac{k\sigma_1}{2}\right). \tag{66}$$

Note that as $\epsilon \to 0$, $k \to 0$ and $\lambda = 2\pi/k \to \infty$.

Figure 3 shows the result of choosing the possible solution $\gamma_2 = \gamma_{2+}$ in (59b) for the same γ_1, and σ_1^2/σ_2^2, as in the example shown in Fig. 1. Note that a steadily evolving rarefaction wave forms.

Figure 4 shows the evolution of an initially localized arca bulgc with $\gamma(x,0) = 0$. Triangular-shaped compression waves evolve moving to the left and right, each consisting of a shock or vortex breakdown followed by a rarefaction wave with oscillation. Figure 5 shows a continuation of the flow of Fig. 4 for the right traveling wave. Also shown is the solution to the hyperbolic equations (47) corresponding to the long-wavelength approximation. The solution based on this approximation reliably predicts the location of the wave and the waveform of the mean disturbance. The width and height of the mean wave appear to be proportional to $t^{1/2}$ and $t^{-1/2}$, as expected. A close examination of the "shock" in the numerical solution of the hyperbolic equations reveals that the shock is spread over two to three Lagrangian particles followed by an overshoot of about 20% of the shock jump. In contrast, for example, the two successive peaks in the solution to the full equations, are separated by 18 particles at $t = 300$ in Fig. 5 (also see Fig. 6).

We believe that the first few successive peaks in γ, as shown in Fig. 5, correspond to multiple vortex breakdowns observed in some axisymmetric experiments[18] and computations.[19,20] To look for flow reversals on the axis in a steady frame, we computed the axial velocity on the centerline using

$$u(0,x) = \frac{1}{4}\int_{-\infty}^{\infty} \frac{\sigma^2(x')\gamma(x')dx'}{[(x-x')^2+\frac{1}{2}\sigma^2(x')]^{3/2}},$$

which is consistent with approximations (62) and (63), and subtracted from this result the speed of the wave c. The result is shown in Fig. 6 along with the core shape and centerline. Note the region of flow reversal approximately 2.0 in length followed by another reversal that is miniscule in size. Larger initial bulges, for example, will yield clearly two or more regions of flow reversal.

If one starts with a localized distribution of γ with $\sigma^2(x,0) = \text{const}$, a triangular compression wave moves to the right (left) for a positive (negative) initial pulse of γ

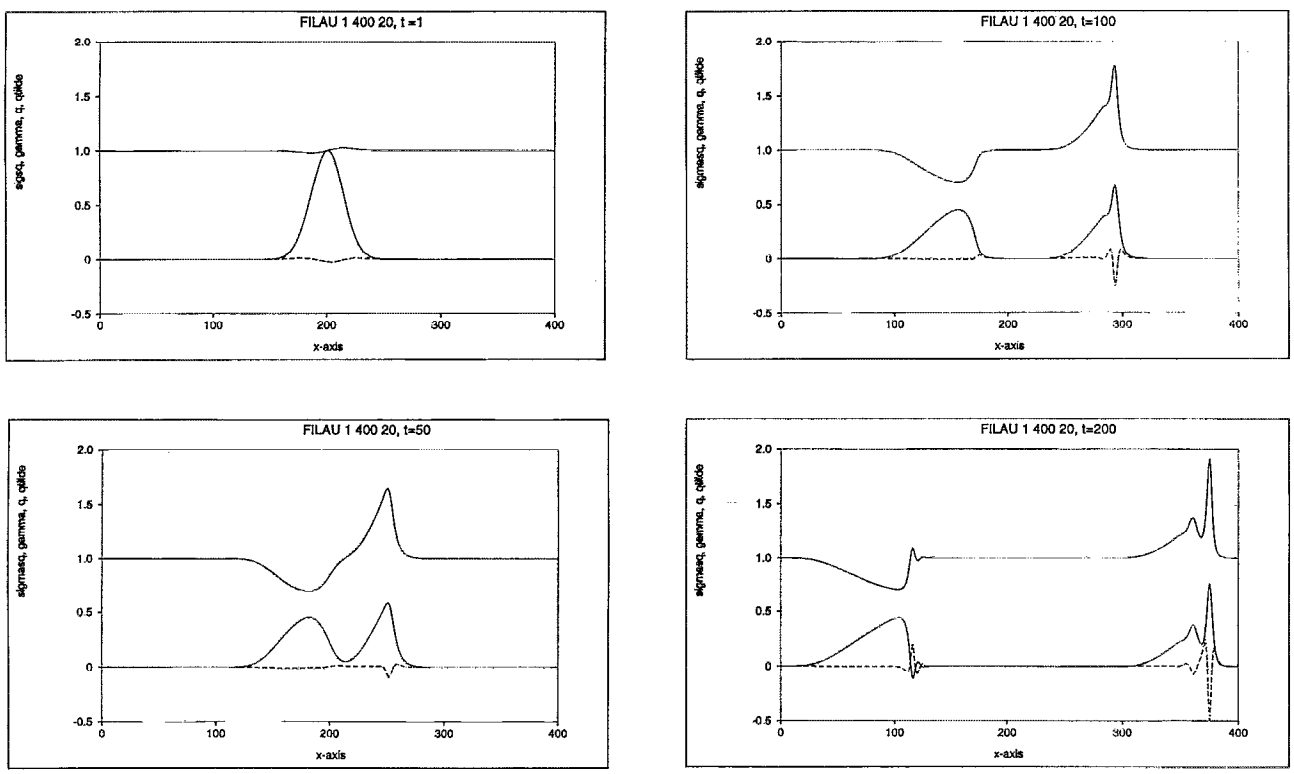

FIG. 7. Evolution of a localized distribution in γ. Here $\sigma^2(x,0) = 1$, $\gamma(x,0) = \exp[-(x-200)^2/400]$. The legend is the same as in Fig. 1.

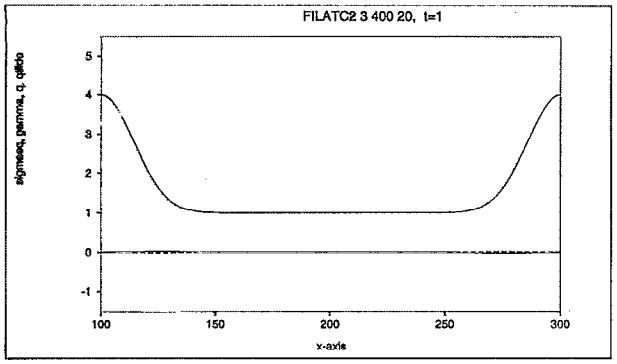

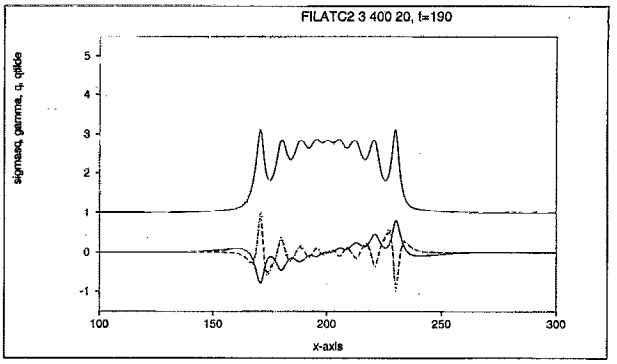

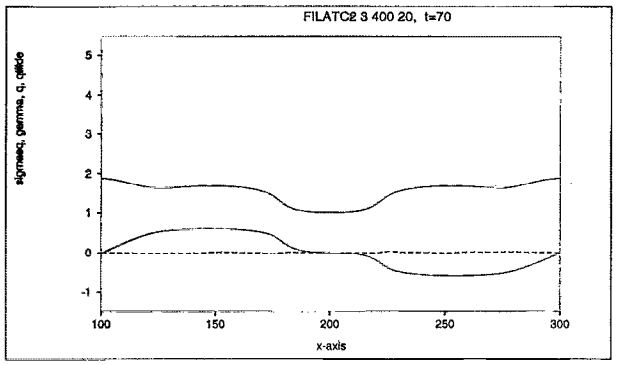

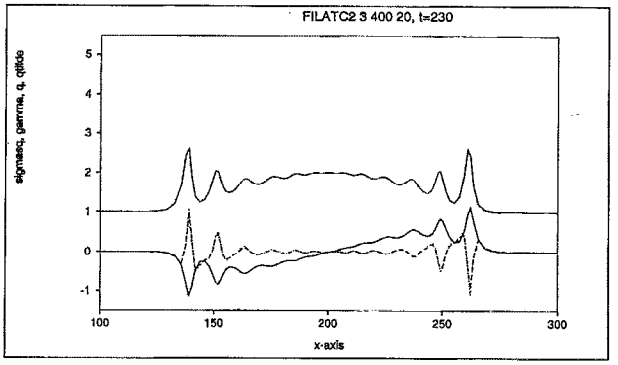

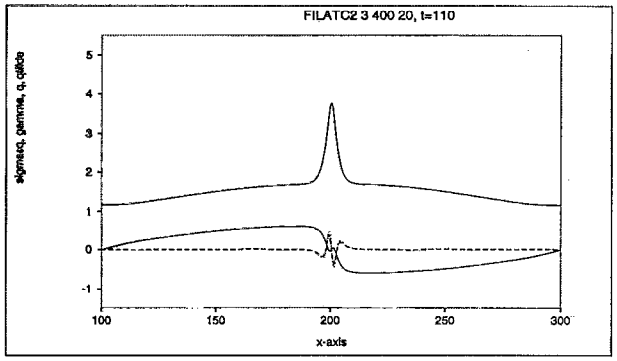

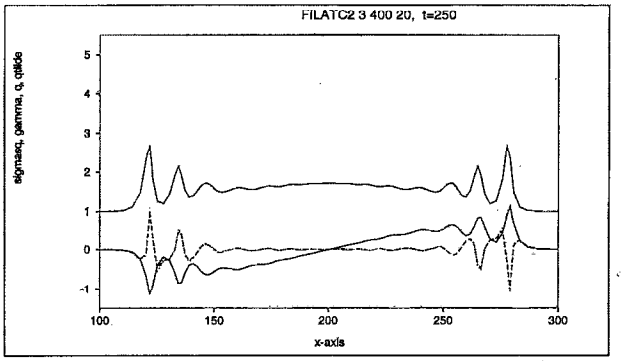

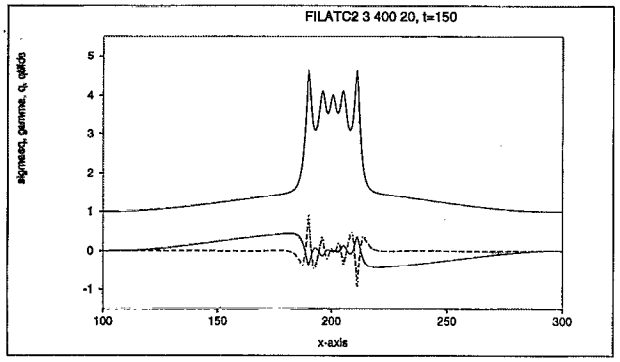

FIG. 8. Evolution of two area bulges. Symmetry conditions at $x=100$ and 300. The legend is the same as in Fig. 1. Here $\sigma^2(x,0)=1+3\exp[-(x-100)^2/200]+3\exp[-(x-300)^2/200]$, and $\gamma(x,0)=0$.

and a triangular expansion wave, a rarefaction wave *leading* a vortex breakdown moves to the left (right). As shown in Fig. 7, we have computed such a case to correspond with the one computed by LA (Fig. 2). The results are qualitatively the same, except for the oscillations found in the present results.

Finally, we compute the collision of two compression waves. Such an interaction will occur, for example, between two initial area bulges, as shown in Fig. 8. As seen, the collision itself excites the oscillatory behavior corresponding again to sequences of vortex rings.

VI. CONCLUSION

We characterize area and axial flow variations along vortex tubes in terms of the square of a width parameter in assumed radial distributions of vorticity and of a circulation per unit length of azimuthal vorticity, respectively. For the case of axisymmetric flows, we derive dynamical equations for these two quantities by enforcing the angular momentum integral (over an axial plane) equation and the azimuthal vorticity integral equation. The distribution of azimuthal vorticity is not assumed independently, but is

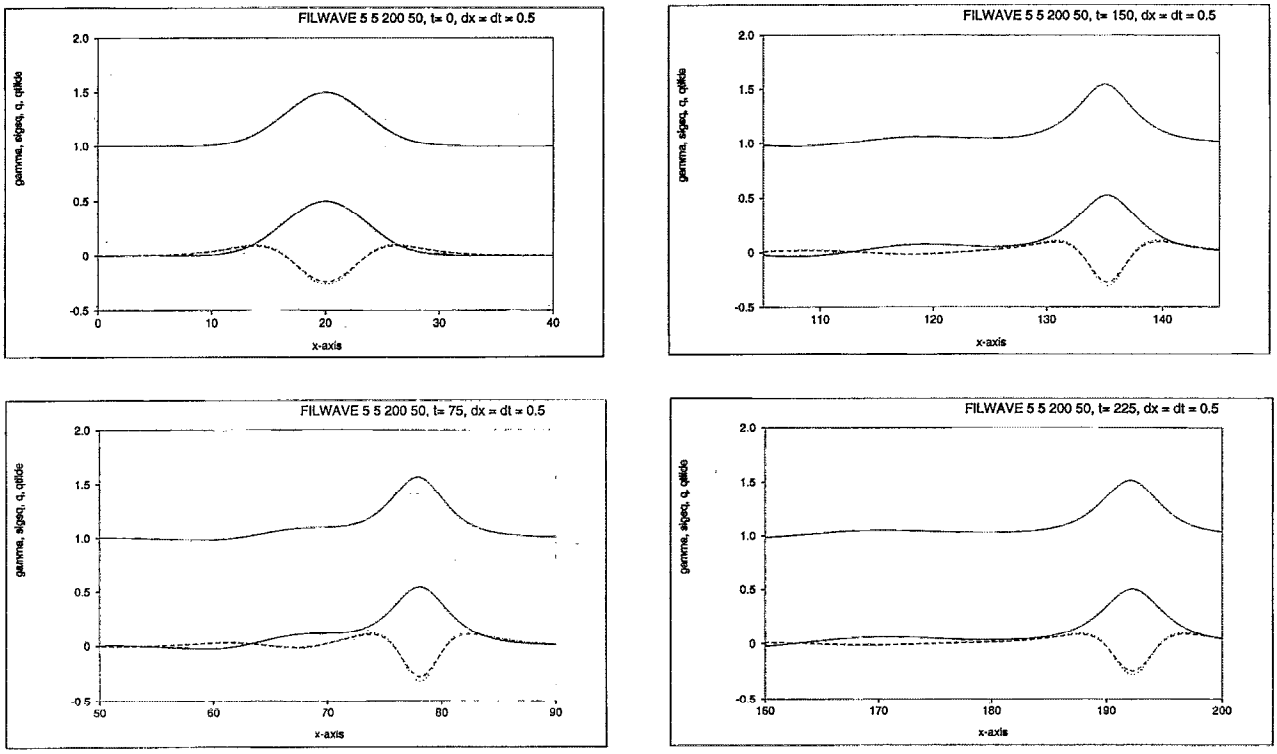

FIG. 9. Evolution of a localized distribution in γ and σ^2. Here $\gamma(x,0)=0.5\exp[-(x-20)^2/25]$, $\sigma^2(x,0)=1+\gamma(x,0)$; $\Delta t=0.5$, initial, $\Delta x=0.5$.

determined from the assumed distribution of axial vorticity. This restricts the applicability of the method, but enhances its accuracy, as seen, for example, by comparison with exact linear theory. For long waves the equations are nonlinear hyperbolic, but, in general, the equations are nonlocal because of the contribution of azimuthal vorticity to the axial and radial velocities at a distance through the Biot–Savart law.

Initial disturbances on a rectilinear vortex tube evolve into wave patterns generally associated with ID compressible gas flow or shallow water waves, i.e., shocks or vortex breakdowns and rarefaction waves, except that on the subcritical side of a wave oscillatory motion is usually observed because the dissipation mechanism of shocks is not available.

The phenomenon of nonlinear traveling waves needs further study, in particular, solitary waves. The relationship between these waves the steady, nonlinear waves computed from the Bragg–Hawthorne equation[21] would be of interest. We believe that the present theory will admit such waves, as evidenced by our preliminary computation shown in Fig. 9. Extension of the analysis to vortex tubes moving as three-dimensional space curves would be useful, especially considering that axisymmetrical or bubble-type vortex breakdown usually involves substantial time-dependent, three-dimensional components.[22]

ACKNOWLEDGMENT

The work was supported by the Applied Hydrodynamics Research Program of the Office of Naval Research under Grant No. N00014-92-J-1189.

APPENDIX: DETERMINATION OF $\tilde{K}$

For the case of a solid-body rotation core, ζ_1 is given by (18a), so that (44) becomes

$$\begin{aligned}\tilde{K}(x,y)&=4\int_0^1 z^3 Q_2[(x^2+z^2y^2)^{1/2}]\,dz\\&=\frac{4}{y^4}\int_x^{\sqrt{x^2+y^2}}(t^3-tx^2)Q_2(t)\,dt\\&=\frac{4}{y^4}\{R_3(\sqrt{x^2+y^2})-R_3(x)\\&\quad -x^2[R_1(\sqrt{x^2+y^2})-R_1(x)]\},\end{aligned}$$

where

$$R_i(x)=\int_0^x t^i Q_2(t)\,dt,\quad i=1,3.$$

From (10b) and (18a), we find that

$$R_1(x)=\begin{cases}\dfrac{4}{3\pi}-\dfrac{\sin^{-1}x}{2\pi x}-5\dfrac{\sqrt{1-x^2}}{6\pi}+\dfrac{x^2\sqrt{1-x^2}}{3\pi} & (x<1),\\ \dfrac{4}{3\pi}-\dfrac{1}{4x} & (x>1),\end{cases}$$

and

$$R_3(x)=\begin{cases}8\dfrac{\sqrt{1-x^2}-1}{15\pi}+\dfrac{x\sin^{-1}x}{2\pi}-\dfrac{x^2(7-6x^2)\sqrt{1-x^2}}{30\pi} & (x<1),\\ \dfrac{x}{4}-\dfrac{8}{15\pi} & (x>1).\end{cases}$$

[1]A. Leonard, "Computing three-dimensional incompressible flows with vortex elements," Annu. Rev. Fluid Mech. **17**, 523 (1985).
[2]J. E. Martin and E. Meiburg, "Numerical investigation of three-dimensionally evolving jets subject to axisymmetric and azimuthal perturbations," J. Fluid Mech. **230**, 271 (1991).
[3]G. S. Winckelmans and A. Leonard, "Contributions to vortex particle methods for the computation of three-dimensional incompressible unsteady flows," J. Comput. Phys. (in press).
[4]D. W. Moore and P. G. Saffman, "The motion of a vortex filament with axial flow," Philos. Trans. R. Soc. London Ser. A **272**, 403 (1972).
[5]S. E. Widnall and D. B. Bliss, "Slender-body analysis of the motion and stability of a vortex filament containing an axial flow," J. Fluid Mech. **50**, 335 (1971).
[6]T. S. Lundgren and W. T. Ashurst, "Area-varying waves on curved vortex tubes with application to vortex breakdown," J. Fluid Mech. **200**, 283 (1989).
[7]J. S. Marshall, "A general theory of curved vortices with circular cross-section and variable core area," J. Fluid Mech. **229**, 311 (1991).
[8]S. Leibovich, "Weakly non-linear waves in rotating fluids," J. Fluid Mech. **42**, 803 (1970).
[9]Lord Kelvin, "Vibrations of a columnar vortex," Philos. Mag. **10**, 155 (1880).
[10]V. Krishnamoorthy, "Vortex breakdown and measurements of pressure fluctuation over slender wing," University of Southampton Ph.D. thesis, 1966.
[11]G. B. Whitham, *Linear and Nonlinear Waves* (Wiley, New York, 1974).
[12]P. D. Lax, "Hyperbolic systems of conservation laws and the mathematical theory of shock waves," *Regional Conference Series in Applied Mechanics* (SIAM, Philadelphia, PA, 1972), Vol. 11.
[13]G. L. Brown and J. M. Lopez, "Axisymmetric vortex breakdown Part 2. Physical Mechanisms," J. Fluid Mech. **221**, 553 (1990).
[14]T. B. Benjamin, "Theory of the vortex breakdown phenomenon," J. Fluid Mech. **14**, 38 (1962).
[15]T. B. Benjamin, "Some developments in the theory of vortex breakdown," J. Fluid Mech. **28**, 5 (1967).
[16]B. Fornberg and G. B. Whitham, "A numerical and theoretical study of certain nonlinear wave phenomena," Philos. Trans. R. Soc. London Ser. A **289**, 373 (1978).
[17]T. B. Benjamin and M. J. Lighthill, "On cnoidal waves and bores," Proc. R. Soc. London Ser. A **224**, 448 (1954).
[18]M. P. Escudier, "Vortex breakdown: Observations and explanations," Prog. Aerosp. Sci. **25**, 189 (1988).
[19]J. M. Lopez, "Axisymmetric vortex breakdown Part 1. Confined swirling flow," J. Fluid Mech. **221**, 533 (1990).
[20]P. S. Beran and F. E. C. Culick, "The role of non-uniqueness in the development of vortex breakdown in tubes," J. Fluid Mech. **242**, 491 (1992).
[21]S. Leibovich and A. Kribus, "Large amplitude wavetrains and solitary waves in vortices," J. Fluid Mech. **216**, 459 (1990).
[22]S. Leibovich, "The structure of vortex breakdown," Annu. Rev. Fluid Mech. **10**, 221 (1978).